PCCP

Hydrogen bond dynamics and conformational flexibility in antipsychotics

Journal:	*Physical Chemistry Chemical Physics*
Manuscript ID	CP-ART-05-2019-002456.R1
Article Type:	Paper
Date Submitted by the Author:	11-Jun-2019
Complete List of Authors:	PEREIRA, JOSE; University of Copenhagen, The Niels Bohr Institute Eckert, Juergen; University of South Florida, Department of Chemistry Rudic, Svemir; Rutherford Appleton Laboratory, Yu, Dehong; Bragg Institute, Mole, Richard; Bragg Institute Tsapatsaris, Nikolaos; European Spallation Source ESS Bordallo, Heloisa; Kobenhavns Universitet Niels Bohr Instituttet,

SCHOLARONE™
Manuscripts

ARTICLE

Hydrogen bond dynamics and conformational flexibility in antipsychotics

Received 00th January 20xx,
Accepted 00th January 20xx

DOI: 10.1039/x0xx00000x

Jose E. M. Pereira,*[a] Juergen Eckert,[bc] Svemir Rudic,[d] Dehong Yu,[e] Richard Mole,[e] Nikolaos Tsapatsaris, [af] and Heloisa N. Bordallo. [af]

Effective treatment of disorders of the central nervous system can often be obtained by using bioactive molecules of similar moiety to those known to be effective. A better understanding of the solid-state characteristics of such molecules could thereby create new opportunities for research on pharmaceutical preparations and drug prescriptions, while information of their rich intramolecular dynamics may well add an important aspect in the field of in-silico drug discovery. We have therefore investigated three different antipsychotic drugs: haloperidol ($C_{21}H_{23}ClFNO_2$, HAL), aripiprazole ($C_{23}H_{27}Cl_2N_3O_2$, APZ) and quetiapine hemifumarate ($C_{21}H_{25}N_3O_2S \cdot 0.5C_4H_4O_4$, QTP) based on similarities either in their structures, hydrophobic and hydrophilic moieties, or in their mode of action, typical or atypical. Our aim was to test the structural and molecular stability of these three different antipsychotics. To this end, we compared the molecular vibrations observed by inelastic neutron spectroscopy for these systems with those from theoretical periodic calculations of the crystalline antipsychotics using the Vienna *Ab initio* Simulation Package (VASP). While most of the observed features in the lattice region were reasonably well represented by the calculations, the spectra overall were relatively complex, so that traditional assignment procedures for the approximately 600 normal modes in the unit cell were not possible. These results indicate that in the search for new drug candidates not only analysis of the flexibility of the receptor, but also the dynamics of the active molecules play a role in improving the prediction of binding affinities.

.

Introduction

The market for antipsychotic drugs is one of the largest in the pharmaceutical industry, valued in 2015 at USD 11.7 billion[1]. These drugs are G-protein coupled receptors (GPCRs) ligands whose binding sites can accommodate many different ligands, including agonists and antagonists[2,3] A great deal of pharmacological and bioanalytic information about these drugs is available[4–7]. By contrast not much is known about their solid-state properties. For instance, X-ray diffraction data of the structures of the various polymorphs are generally patented, and only few papers on infrared (IR) and Raman scattering (RS) of these particular drugs can be found in the open literature [8–16] despite the fact that these techniques have been widely employed to characterize pharmaceutical compounds[17–19]. As there is a general lack of understanding of the conformational habit of these molecules we have combined inelastic neutron scattering (INS) and density functional theory (DFT) calculations to obtain a stringent test of the molecular conformation of three different antipsychotics, haloperidol (HAL), aripiprazole (APZ) and quetiapine hemifumarate (QTP, marketed by AstraZeneca under the brand name Seroquel), whose structures are represented in Figure 1.

HAL, APZ and QTP molecules were selected because they represent different generations of antipsychotics drugs and also because their function has been widely discussed. In solid state HAL is a flexible molecule which contains a central cyclohexane ring with a tertiary amine nitrogen, an alcoholic hydroxy, and ketone functionality. In their crystalline form the molecules are assembled by means of strong O–H···N hydrogen bonds between the tertiary amine nitrogen and the hydroxy functionality and crystallize in monoclinc space group $P2_1/n$ [20]. APZ, on the other hand, has a rather simple molecular structure with aliphatic chains and saturated rings which makes this molecule susceptible to polymorphism. Patents show that APZ exhibits not only polymorphism, but also exists as pseudopolymorphs or in amorphous form. Detailed investigations of their conformational habits and their stability were described by Ayala *et al*. [9]and Braun *et al*. [13]. Finally for QTP five solid-state forms

[a] *The Niels Bohr Institute, University of Copenhagen, DK-2100, Copenhagen, Denmark.*
[b] *Department of Chemistry and Biochemistry, Texas Tech University, Lubbock, TX 79409-1061, USA.*
[c] *Theoretical Division, Los Alamos National Laboratory, Los Alamos, NM 87545, USA*
[d] *ISIS Facility, STFC, Rutherford Appleton Laboratory, Chilton, Didcot OX11 0QX, United Kingdom*
[e] *Australian Center for Neutron Scattering, Australian Nuclear Science and Technology Organization, Lucas Heights, 2233 NSW, Australia.*
[f] *European Spallation Source ESS ERIC, PO Box 176, SE-221 00 Lund, Sweden*
†Electronic Supplementary Information (ESI) available: Animations resulting from the DFT calculations, XRPD, RS and additional DSC data together with comparisons of the experimental and calculated spectra as well as a table with the assignment of the main vibrational modes are provided in the supplementary information. See DOI: 10.1039/x0xx00000x

have been reported to date: three polymorphs and two amorphs[19]. QTP generally contains many impurities, that can be isolated by means of NMR, IR, mass spectrometry (MS) liquid chromatography coupled with tandem MS (LC-MS/MS)[21,22]. The presence of these unwanted chemicals, even in small amounts, may influence the efficacy and safety of the pharmaceutical products. From the pharmacological point of view HAL is a typical antipsychotic agent frequently used to treat schizophrenia. It works by blocking receptors for the chemical dopamine in the brain causing neuron apoptosis. APZ and QTP, on the other hand, are atypical antipsychotics which bind to several different neurotransmitter receptors[23,24]. From a clinical point of view is widely accepted that the D_2 dopamine receptor (DRD2) is the primary target for both typical and atypical antipsychotics, however there is no clear evidence that one type is more effective or better tolerated than the other[5–7,25]. It is also believed that HAL has high affinity dopamine D_2 receptor antagonism, while the actions of APZ have been ascribed alternately to either D_2 partial agonism or D_2 functional selectivity. On the other hand, QTP is considered a weak D_2 antagonist as well as a drug that presents "rich" pharmacology as a result of it effectiveness with decreased side effects[26]. In fact, the main difference in the mechanism of action is related to the strength of binding which in turn changes the dissociation constant, which is lower than that of dopamine in HAL and higher in QTP[27]. This agrees with the idea that protein-ligand interactions are closely related to binding affinity. However, because the exact nature of the multiple receptor actions is critical but not well understood, it has been suggested that the term "dirty" drug should be used instead of "rich" pharmacology[28] .

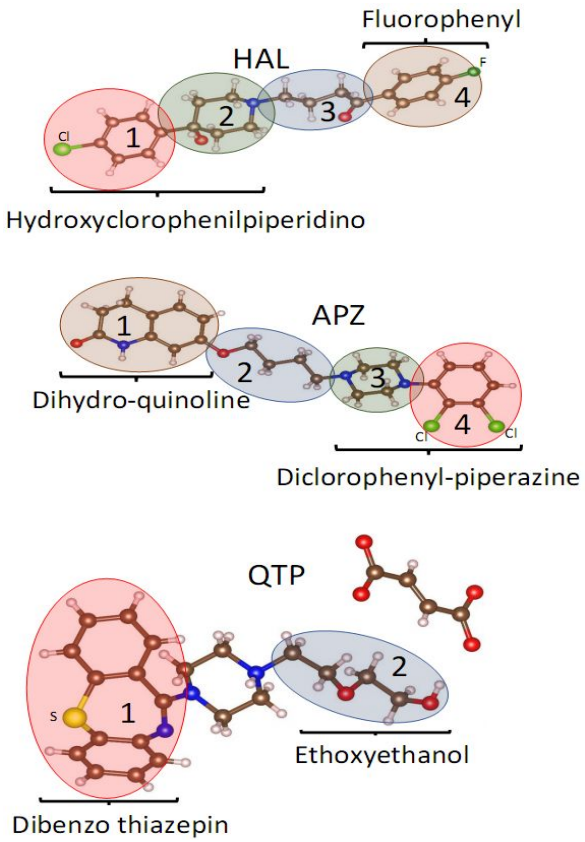

Fig. 1 Molecular structure of HAL ($C_{21}H_{23}ClFNO_2$), APZ ($C_{23}H_{27}Cl_2N_3O_2$) and QTP ($C_{21}H_{26}N_3O_2S^+ \cdot 0.5C_4H_2O_4^{2-}$)

In this work, the crystal structures of the three biomolecules were first confirmed by X-ray powder diffraction (XRPD), while RS was used to check the polymorphic form of APZ prior to carrying out the INS studies and DFT calculations. Structural transformations and purity were determined using differential scanning calorimetry (DSC) and thermogravimetric analysis coupled with Fourier transform infrared spectroscopy (TGA-FTIR).

Experimental details

Antipsychotic samples

Powder samples of APZ ($C_{23}H_{27}Cl_2N_3O_2$) and QTP ($C_{21}H_{25}N_3O_2S \cdot 0.5C_4H_4O_4$) were purchased from CHEMOS GmbH, while HAL ($C_{21}H_{23}ClFNO_2$) was acquired from Sigma Aldrich. All samples were used without further purification.

X-rays powder diffraction

XRPD was performed at ambient conditions using a Bruker D8 Advance diffractometer with Cu Kα radiation (1.5418 Å) in θ/θ geometry to confirm the purity as well as the polymorphic structure of each sample, Figure S1.

Raman scattering

Raman spectra for APZ and HAL were collected at room temperature using a RamanRxn1 spectrometer with CCD detector (Kaiser Optical Systems), Figures S6 and S7.

Calorimetric studies

The purity of each sample was further checked by the thermogravimetric analysis instrument PERSEUS TG 209 F1 Libra from NETZSCH coupled with a Fourier transform infrared spectrometer by BRUKER Optics Inc. (TGA-FTIR). Changes in the mass of the sample as a function of temperature observed by TGA gives insight in the sample decomposition, while the slope of the mass loss indicates how rapidly the decomposition occurs. The gases released during the heating process for each sample are characterized by the attached FTIR Spectrometer to determine the nature of the decomposition products. When combined with differential scanning calorimetry (DSC) (NETZSCH DSC 214 *Polyma*) these measurements give a complete picture of thermal effects on the crystalline stability of these bioactive molecules.

Samples were placed in alumina crucibles for the TGA experiments and heated from room temperature (RT) to 300 °C at a constant heating rate of 10 °C/min. A stream of nitrogen flowing at 20 ml/min was used throughout the experiment. FTIR spectra of the evolved gases were recorded every 3 °C to facilitate the understanding of the decomposition process.

This journal is © The Royal Society of Chemistry 20xx

Please do not adjust margins

DSC data were collected on samples sealed in aluminium crucibles, finally, the spectra were converted to the incoherent dynamic

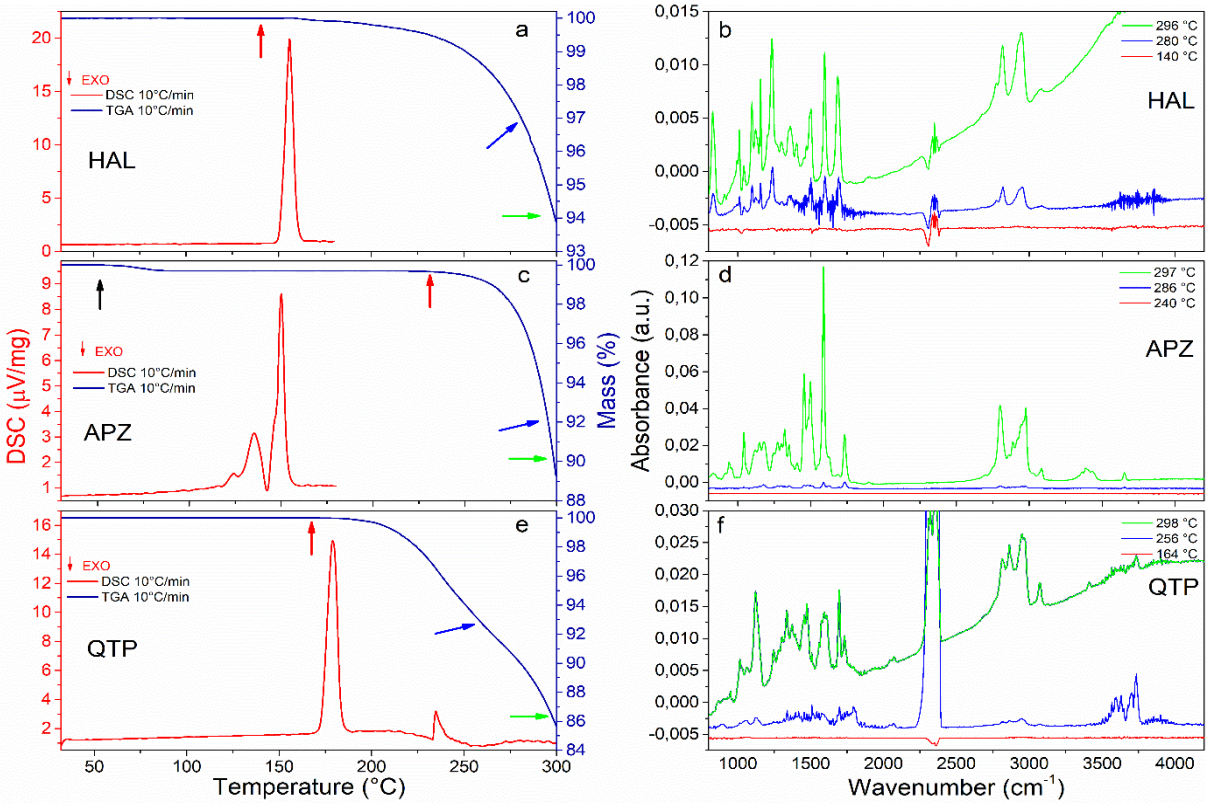

FIG. 2 TGA-FTIR and DSC data for haloperidol (HAL), aripiprazole (APZ), and quetiapine hemifumarate (QTP). The left side of the figure shows the TGA and DSC curves while on the right side the FTIR collected during the heating process is shown. The arrows in the left side correspond to the specific temperature at which respective FTIR data have been depicted. The black arrow in (c) indicates a dehydration in APZ.

and placed in a nitrogen atmosphere purged at 40 ml/min. An empty crucible was used as reference material. The instrument was calibrated with indium as a standard. Heating rates between 2 and 15 °C/min were used for all the samples, see Figure S2. HAL and APZ were measured between RT (25 °C) and 180 °C, while data for QTP were collected up to a temperature of 300 °C.

Inelastic neutron scattering (INS)

The dynamics of polycrystalline antipsychotic compounds were studied by INS vibrational spectroscopy using the spectrometers PELICAN[29] at the Australian Nuclear Science and Technology Organisation - ANSTO (Australia) and TOSCA[30] at the ISIS Neutron and Muon Source at the Rutherford Appleton Laboratory (United Kingdom). The INS data were compared and interpreted using the simulated spectra obtained from DFT calculations described below.

PELICAN is a cold neutron time-of-flight spectrometer that gives access to vibrational motions in the energy range 0 – 40 meV. With an incident wavelength of 4.72 Å, corresponding to an incident energy of 3.61 meV, excitations are measured by energy gain of the neutron, or the energy loss of the sample, i.e. on the anti-Stokes side of the spectra. The data were collected at temperatures of 60 K, 100 K, 150 K, 200 K, 250 K and 300 K and processed using the Large Array Manipulation Program (LAMP)[31] as follows. The spectra were first normalized to a vanadium standard, followed by subtraction of the spectrum of an empty sample holder to correct for background, and structure factor, S(Q, ω), where Q is the magnitude of the scattering wave vector and ω is the energy transfer. This scattering function is dominated by vibrational motions of the hydrogen atoms and correlated to the generalized density of state (GDOS, $\mathrm{G}(\hat{\theta},\omega)$), and in turn to the thermal populations of the excitations. Here it is interesting to mention that INS can also be considered an important tool in the development of deuterated pharmaceuticals which in some cases are superior to their protonated counterparts[32,33]. Direct information on the variations of intermolecular and intramolecular distances might shed light on how and if the strength of these interactions influences the ligand binding to the receptor. Information contained in S(Q, ω) was derived as follows:

$$\mathrm{G}(\hat{\theta},\omega) = \frac{S(\hat{\theta},\omega)}{Q^2(\hat{\theta},\omega)} B(\omega, T), \tag{1.2}$$

$S(\hat{\theta},\omega)$ is the scattering function calculated at each energy transfer value for the averaged scattering angle, $\hat{\theta}$, obtained by summing the signal from the first to the last considered detector, θ_i, as:

$$S(\hat{\theta},\omega) = \frac{1}{N_D}\sum_i S_i(\theta_i,\omega), \tag{1.2}$$

$$B(\omega, T) = \hbar\omega\left(1 - e^{-\hbar\omega/kT}\right), \tag{1.3}$$

Please do not adjust margins

B(ω,T) is a function accounting for the population of the vibrational modes at the temperature, *T* [34]. The temperature dependence of the GDOS will give rise to broadening in the harmonic motions of the molecular groups in HAL, APZ and QTP.

TOSCA is an indirect geometry time-of-flight neutron spectrometer with a fixed final energy of the neutrons for observing vibrational spectra in neutron energy loss. The instrument covers the entire frequency range for molecular vibrations. INS spectra for all samples were recorded at 10 K and converted to the incoherent dynamics structure factor, S(Q, ω) using Mantid software[35].

DFT computational details

The INS spectra were generated from periodic calculations of crystalline antipsychotics using the Vienna *Ab initio* Simulation Package (VASP) with the Perdew–Burke–Ernzerhof (PBE) functional along with Vanderbilt ultrasoft pseudopotentials[36], and with the plane wave kinetic energy cutoff at 450 meV. Additional periodic calculations were carried with a 4 x 4 x 4 Monkhorst-Pack mesh of k-points[37] to improve the agreement at lower frequencies. The atomic coordinates were optimized with the unit cell fixed at the experimental values, followed by harmonic frequency calculations. The resulting vibrational amplitudes and frequencies were used to derive a simulated INS spectrum with the aCLIMAX software[38]. Energies of the single molecule were calculated with the same methodology by placing each molecule in a large box surrounded by vacuum. The lattice energy was then estimated from the difference between the isolated molecule energy and that of the same molecule in the crystal structure.

Results and discussion

Structural characterization of HAL, APZ and QTP at room temperature

The XRPD data, (results shown in the supplementary information, Figure S1), show diffraction patterns for HAL and APZ which are in agreement with the previous results from the Cambridge Crystallographic Data Centre (CCDC) files 150416 (monoclinic form, space group P $2_1/n$)[39] and 690585 (triclinic form III, space group P-1)[13]. A comparison of the Raman spectrum of APZ collected at room temperature (results also shown in the supplementary information, Figure S6) from 720 to 790 cm^{-1} and between 1000 and 1070 cm^{-1} with the data reported in Ref [13] suggests that the kinetically highly stable Form III is predominant. The data for QTP are consistent with those previously reported in file number 2206876 from Crystallography Open Database (monoclinic form, space group $P2_1/c$)[10].

Structural stability determined by thermal analysis

DSC results for HAL, APZ and QTP are shown in Figures 2a, 2c and 2e, as well as in Figure S2. Clear and sharp endothermic events related to the melting points at 155 and 178 °C are observed in the DSC data for HAL and QTP, respectively. The weak endothermic event at 120 °C for APZ is related to the loss of hydration water and correlates directly with the weak mass loss observed in the TGA curve above 90 °C as indicated by the black arrow in Figure 2c. The shape of the DSC curve for APZ indicates that the kinetically highly stable room temperature triclinic form III (space group P-1) is mixed with form I (monoclinic, $P2_1$)[13]. Gases evolved during the decomposition steps, indicated by arrows in the TGA curves, give rise to absorption peaks in the infrared spectra (Figures 2b, 2d and 2f), where the strong bands observed between 1450 and 1600 cm^{-1}, and between 2700 and 3100 cm^{-1} are likely from the aromatic rings mixed with C H and C N vibrations, and those and between 2700 and 3100 cm^{-1} to C-H stretching modes.

Additional detailed DSC measurements using the same heating rate for each compound, presented in the supplementary information, see Figures S3-S5, lead to the conclusion that HAL maintains its stable monoclinic crystalline form after a series of heating processes, while APZ changes its structure after the first heating cycle, and the metastable form III predominates thereafter. QTP degrades since it loses hemifumarate ($C_4H_2O_4$) which is needed for stabilizing the structure. This is further confirmed by the presence of a second endothermic transition at about 235 °C in the DSC data (Figure 2e) and the observation of the strong CO_2 asymmetric stretch at 2300 cm^{-1} in the infrared spectrum at 255 °C (Figure 2f). Our calorimetric data agree well with previous reports [40,41] and confirm the polymorphic form for each sample in conjunction with the XRPD and RS results.

Vibrational spectra of HAL, APZ and QTP as function of temperature

The most fundamental difference between optical spectroscopy techniques, such as RS, IR and INS, lies in the nature of the interaction between the probe and the sample. Whereas photons interact with the electron density, neutrons are scattered by the atomic nuclei, so that there are no symmetry-based selection rules for INS spectra. Moreover, neutrons have mass and consequently the scattering process also involves momentum transfer. Neutrons can be scattered with or without a change in their energy, i.e. inelastically or elastically, and this process can be coherent or incoherent. The coherent part of the inelastic scattering gives information about collective lattice vibrations, typically at energies less than 40 meV, while internal molecular vibrations at higher frequency are mainly observed in the incoherent inelastic scattering involving motions of H atoms. INS intensities of vibrational bands are a sensitive test for validation of force fields in MD simulations, and of methodology used in DFT calculations[42].

INS spectra collected on PELICAN (Figures 3-5) in neutron energy gain are considerably broadened at higher temperatures as a result of the Debye–Waller factor, which is particularly noticeable in APZ between 200 and 300 K. Furthermore, the observed experimental intensities of some bands are found to increase strongly upon cooling in all the samples (Figures 3, 4 and 5), a feature common to orientationally disordered crystals[43,44].

This journal is © The Royal Society of Chemistry 20xx

Please do not adjust margins

Comparisons of the experimental INS spectra for HAL, APZ and QTP with those calculated by DFT are intended to provide information about the flexibility of the molecular groups in each sample and to connect this flexibility to the stability of the crystalline structures. Indeed, the calculation does seem to account for most of the observed features in the lattice region, despite the fact that it does not include the appropriate reciprocal space average over full phonon dispersion curves. For instance, we note that the INS spectra collected using TOSCA at 10 K are quite well reproduced by the theoretical results, while the energy gain spectra at 100 K for HAL (cooling cycle on PELICAN) mainly appear to correspond to the calculated results below 20 meV. However, considering that the spectra are relatively complex, as a result of the low symmetry of these molecules and their large unit cells, standard assignments were not possible. Actually, in these systems, a single INS low frequency band may consist of several normal modes. Vibrational features can therefore be mainly described by viewing animations of the normal modes rather than by unambiguous traditional assignments, even in cases where the agreement between calculated and experimental data is sufficiently good. Consequently, descriptions of the molecular motions involved in the main vibrational bands were achieved by visualizing the molecular vibrations of the modes obtained by VASP using the Jmol software [45] . These features may be better understood by viewing video clips provided in the supplementary information. Following this procedure, our analysis of the vibrational modes in the solid suggests that for APZ and QTP most of the intensity below 40 meV (i.e. ~320

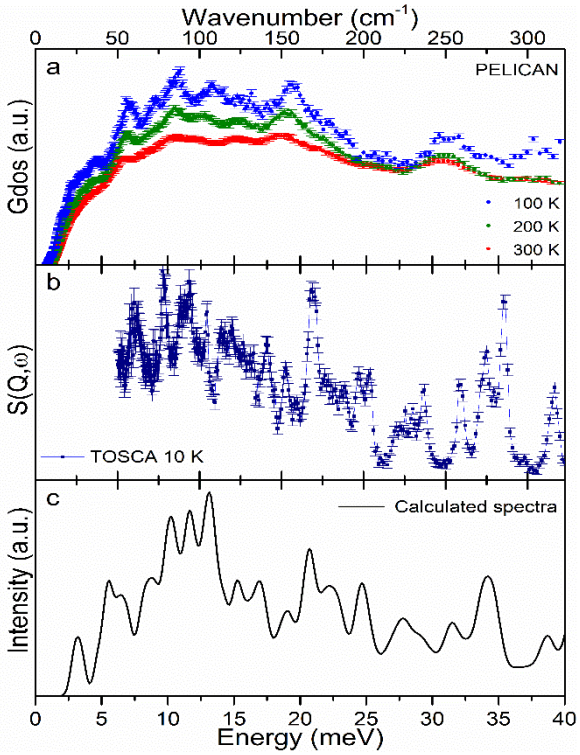

Fig. 4 Experimental and calculated INS data for APZ ($C_{23}H_{27}Cl_2N_3O_2$). (a) Experimental INS data collected using the spectrometer PELICAN at different temperatures. (b) Experimental INS data obtained at 10 K using the TOSCA spectrometer. (c) Calculated INS spectrum using the VASP software.

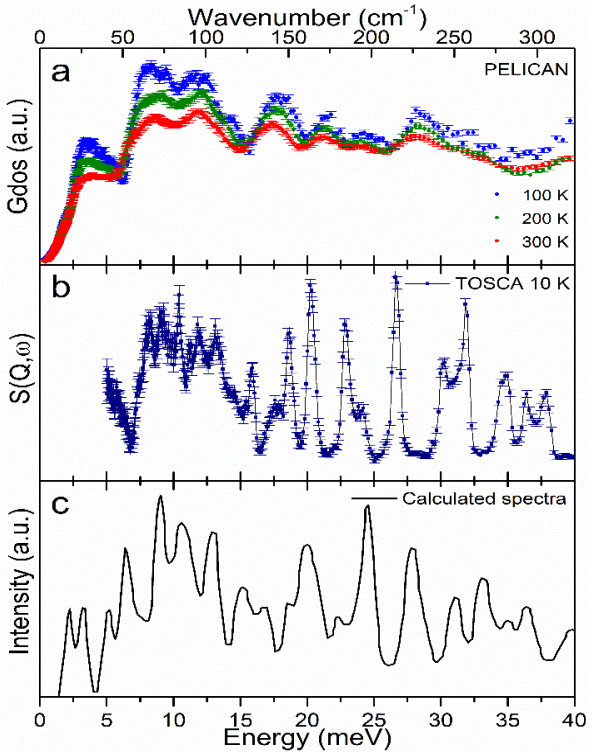

Fig. 3 Experimental and calculated INS data for HAL ($C_{21}H_{23}ClFNO_2$). (a) Experimental INS data collected using the spectrometer PELICAN at different temperatures. (b) Experimental INS data obtained at 10 K using the TOSCA spectrometer. (c) Calculated INS spectrum using the VASP software.

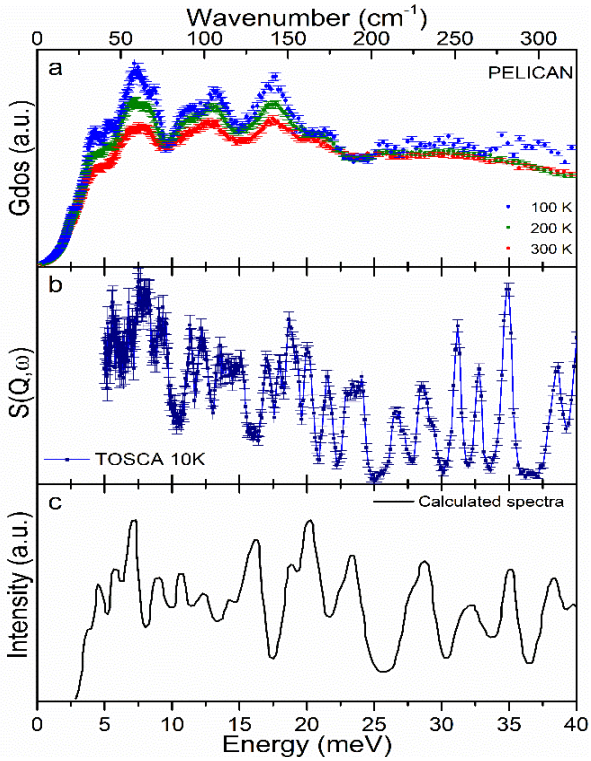

Fig. 5 Experimental and calculated INS data for QTP ($C_{21}H_{25}N_3O_2S \cdot 0.5C_4H_4O_4$). (a) Experimental INS data collected using the spectrometer PELICAN at different temperatures. (b) Experimental INS data obtained at 10 K using the TOSCA spectrometer. (c) Calculated INS spectrum using the VASP software.

cm^{-1}) results from mixed external modes of the molecule in the lattice. Among the most intense bands found in the calculated spectra the mode at 8 meV in HAL can be described in terms of displacements of the hydrogen atoms in the benzene and piperidine rings, while some of the low frequency modes result from deformations of the alkyl group connecting the hydrophobic (hydroxyclorophenylpiperidino) and hydrophilic (fluorophenyl) heads. (denoted as groups 1 and 4, in Figure 1). In the case of APZ the vibrational spectra are relatively well structured. This is an interesting point since form III[13] of this molecule is intrinsically disordered yet kinetically stable. In this sample the observed modes can be described as collective motions of the whole molecule with respect to one another, and mostly dominated by displacements of the diclorophenylpiperazine (denoted as group 3 and 4 in Figure 1) and quinolone (denoted as group 1 in Figure 1) rings. Finally, the main low frequency bands in QTP at 7 and 20 meV arise from a deformation (alternate ring stretch) of the dibenzo thiazepin (denoted group 1 in Figure 1), while the mode at 16 meV results from wagging on the ether group (O) on the ethoxyethanol side chain (denoted as group 2 in Figure 1).

Additional *ab initio* calculations relevant to high frequencies in the Raman and INS spectra were carried out on isolated molecules of APZ and HAL using the Gaussian software[46] along with aCLIMAX[38] for normal mode intensities. Assignments of select high frequency modes are given on Table S1 (see supplementary material). Finally, comparison of the calculations for the isolated molecules modes with that of the crystal shows an overall good agreement. These results are given in the supplementary information, Figures S6-S9.

Conclusions

In the present study we compared one typical (HAL) and two atypical antipsychotic compounds (APZ, QTP), which have shown to be pharmaceutical solids with intriguing and complex dynamical behaviour on the molecular scale. The structural conformation of powder samples of the bulk compounds was characterized by XRPD, RS and calorimetric analysis (DSC and TGA/FTIR). Our results were found to be in accordance with previously published data[10–12]. The molecular vibrational modes in the solids were analysed using INS spectra collected by a thoughtful combination of both indirect- and direct-geometry spectrometers covering a sufficiently broad spectral range with adequate resolution and as a function of temperature. The vibrational spectra were simulated by means of DFT methods both in the gas phase, and in the periodic system. The soft nature of the crystalline lattices creates rich intramolecular dynamics, which results in INS spectra of extreme complexity for the large number of normal modes in the crystal, which makes it impossible to make simple assignments of the observed bands to any particular vibrational mode.

Even if computational methods have the capability to provide atomistic detail to simulate processes of ligand binding to a GPCR, it is often the lowest energy conformation of the ligand which is assumed to be solely responsible for binding and activation of the receptor[47]. It is clear that consideration of ligand receptor flexibility can considerably improve the accuracy of algorithms used to estimate binding affinities between a potential therapeutic drug and its target[48]. However, while the number of available crystal structures of GPCRs has increased considerably[49], an extensive set of crystal structures with different and relevant conformations of the bound and unbound GPCR receptor is not yet fully available[2]. On the other hand, the results described in this manuscript clearly show that small active biomolecules have very complex dynamics, which will hopefully give rise to efforts to add the findings offered by vibrational spectroscopy of low frequency deformations of such molecules to computational tools normally used in the *in-silico* calculations in drug discovery. This approach may provide a new perspective on the understanding of how biomolecular recognition mechanisms and conformational selection account for the dynamic association process of a bioactive drug molecule. While protein flexibility may well be the most important factor in the suitability of binding sites, it is also of great interest to identify how this interaction with the drug molecule is affected by the drug flexibility. It was in fact recently discussed that keeping biomolecules flexible, as opposed to having them rigid when they bind to their receptors, reduces the entropy penalty and thereby creates stronger binding and hence improved drug delivery[50]. One of the most important physicochemical properties for pharmaceutical use of small organic molecules, is their aqueous solubility, which is generally calculated approximately by considering only the experimental melting data. It may therefore be useful to find different approaches to predict lattice energies in order to greatly advance drug design[51]. We have therefore calculated the lattice energies of the three compounds analyzed in this study, and obtained values for APZ (109 kcal/mol) < HAL (235 kcal/mol) < QTP 859 kcal/mol (the latter being much higher because the structure is ionic). The order of the lattice energies follows that of the experimental data for the measured enthalpy of fusion ($\Delta_{fus}H$): ($\Delta_{fus}H$ (APZ) (10 kcal/mol) < ($\Delta_{fus}H$ (HAL) (12 kcal/mol) < ($\Delta_{fus}H$ (QTP) (18 kcal/mol)[13,19,52]. Our results therefore suggest that the predicted lattice energies of APZ HAL and QTP follow the behavior of $\Delta_{fus}H$, and as such the may be an alternative method for predicting solubility behavior.

Conflicts of interest

There are no conflicts to declare.

Acknowledgements

J.E.M.P. thanks José Gadelha da Silva Filho for continuous discussions related to the DFT results. We are grateful to Marianne Lund Jensen for her assistance during the thermoanalysis experiments, to Niels Vissing Holst for his support in the X-rays data collection and to Jiwoong Lee for discussions related to the chemistry of these molecules. The authors thank Ivana Gonzales and Panchapakesan Ganesh for assistance with some of the periodic DFT calculations. J.E.M.P.'s

 This journal is © The Royal Society of Chemistry 20xx

Please do not adjust margins

research was supported through the Brazilian Science Without Borders (Process number 207740/2014-3) program. JE used resources of the National Energy Research Scientific Computing Center (NERSC), a U.S. Department of Energy Office of Science User Facility operated under Contract No. DE-AC02-05CH11231. J.E. would also like to thank the Physics and Chemistry of Materials Group (T-1) at LANL for making computing resources available. The thermoanalysis apparatus used in the work were financed by Carlsbergfondets (grants 2013_01_0589 and CF14-0230). We thank the Danish Agency for Science, Technology, and Innovation for funding the instrument center DanScatt. We acknowledge the support of Rutherford Appleton Laboratory (ISIS Facility) and the Australian Center for Neutron Scattering in providing the neutron research facilities used in this work.

References

1 Antipsychotic Drugs Market Size & Share | Industry Report, 2014-2025, http://www.grandviewresearch.com/industry-analysis/antipsychotic-drugs-market, (accessed 20 November 2017).

2 S. Wang, T. Che, A. Levit, B. K. Shoichet, D. Wacker and B. L. Roth, *Nature*, 2018, **555**, 269–273.

3 L. A. Catapano and H. K. Manji, *Biochim. Biophys. Acta - Biomembr.*, 2007, **1768**, 976–993.

4 G. Zhang, A. V. T. Jr and M. G. Bartlett, *Biomed. Chromatogr.*, 2008, **22**, 671–687.

5 G. W. Arana, *J. Clin. Psychiatry*, 2000, **61 Suppl 8**, 5–11; discussion 12-3.

6 D. S. Cha and R. S. McIntyre, *Expert Opin. Pharmacother.*, 2012, **13**, 1587–98.

7 A. Uçok and W. Gaebel, *World Psychiatry*, 2008, **7**, 58–62.

8 B. D. Robbins, M. Higgins, M. Fisher and K. Over, *J. Psychol. Issues Organ. Cult.*, 2011, **1**, 32–49.

9 A. P. Ayala, S. B. Honorato, J. M. Filho, D. Grillo, M. Quintero, F. Gilles and G. Polla, *Vib. Spectrosc.*, 2010, **54**, 169–173.

10 K. Ravikumar, B. Sridhar, IUCr, C. J., D. J., R. F. C., W. S., C. M. O. and J. N. D., *Acta Crystallogr. Sect. E Struct. Reports Online*, 2005, **61**, o3245–o3248.

11 J. B. Nanubolu, B. Sridhar, V. S. P. Babu, B. Jagadeesh and K. Ravikumar, *CrystEngComm*, 2012, **14**, 4677.

12 G. L. Destri, A. Marrazzo, A. Rescifina and F. Punzo, *J. Pharm. Sci.*, 2011, **100**, 4896–4906.

13 D. E. Braun, T. Gelbrich, V. Kahlenberg, R. Tessadri, J. Wieser and U. J. Griesser, *J. Pharm. Sci.*, 2009, **98**, 2010–2026.

14 S. Jafari, F. Fernandez-Enright and X.-F. Huang, *J. Neurochem.*, 2012, **120**, 371–384.

15 A. Alparone, *Spectrochim. Acta Part A Mol. Biomol. Spectrosc.*, 2011, **81**, 631–639.

16 S. Sagdinc, F. Kandemirli and S. H. Bayari, *Spectrochim. Acta Part A Mol. Biomol. Spectrosc.*, 2007, **66**, 405–412.

17 A. Hédoux, *Adv. Drug Deliv. Rev.*, 2016, **100**, 133–146.

18 S. Wartewig and R. H. H. Neubert, *Adv. Drug Deliv. Rev.*, 2005, **57**, 1144–70.

19 S. Jin, S. Du, Y. Liu, D. Han, Z. Li, K. Li and J. Gong, *J. Chem. Eng. Data*, 2017, **62**, 4144–4153.

20 L. Rajput, *Cryst. Growth Des.*, 2014, **14**, 5196–5205.

21 E. U. Stolarczyk and A. Kutner, *Acta Pol. Pharm.*, **67**, 599–608.

22 E. U. Stolarczyk, L. Kaczmarek, K. Eksanow, M. Kubiszewski, M. Glice and A. Kutner, *Pharm. Dev. Technol.*, 2009, **14**, 27–37.

23 K. Al Jurdi, L. A. Dixit and M. Sajatovic, *Neuropsychiatr. Dis. Treat.*, 2010, **6**, 29–35.

24 A. De Bartolomeis, C. Tomasetti and F. Iasevoli, *CNS Drugs*, 2015, **29**, 773–799.

25 J. Geddes, N. Freemantle, P. Harrison and P. Bebbington, *BMJ*, 2000, **321**, 1371–1376.

26 R. B. Mailman and V. Murthy, *Curr. Pharm. Des.*, 2010, **16**, 488–501.

27 P. Seeman, *Can. J. Psychiatry.*, 2002, **47**, 27–38.

28 B. L. Roth, D. J. Sheffler and W. K. Kroeze, *Nat. Rev. Drug Discov.*, 2004, **3**, 353–359.

29 D. Yu, R. Mole, T. Noakes, S. Kennedy and R. Robinson, *J. Phys. Soc. Japan*, 2013, **82**, SA027.

30 D. Colognesi, M. Celli, F. Cilloco, R. J. Newport, S. F. Parker, V. Rossi-Albertini, F. Sacchetti, J. Tomkinson and M. Zoppi, *Appl. Phys. A Mater. Sci. Process.*, 2002, **74**, s64–s66.

31 D. Richard, M. Ferrand and G. J. Kearley, *J. Neutron Res.*, 1996, **4**, 33–39.

32 G. S. Timmins, *Expert Opin. Ther. Pat.*, 2017, **27**, 1353–1361.

33 C. Schmidt, *Nat. Biotechnol.*, 2017, **35**, 493–494.

34 S. Rols, H. Jobic and H. Schober, *Comptes Rendus Phys.*, 2007, **8**, 777–788.

35 O. Arnold, J. C. Bilheux, J. M. Borreguero, A. Buts, S. I. Campbell, L. Chapon, M. Doucet, N. Draper, R. Ferraz Leal, M. A. Gigg, V. E. Lynch, A. Markvardsen, D. J. Mikkelson, R. L. Mikkelson, R. Miller, K. Palmen, P. Parker, G. Passos, T. G. Perring, P. F. Peterson, S. Ren, M. A. Reuter, A. T. Savici, J. W. Taylor, R. J. Taylor, R. Tolchenov, W. Zhou and J. Zikovsky, *Nucl. Instruments Methods Phys. Res. Sect. A Accel. Spectrometers, Detect. Assoc. Equip.*, 2014, **764**, 156–166.

36 J. P. Perdew, K. Burke and M. Ernzerhof, *Phys. Rev. Lett.*, 1996, **77**, 3865–3868.

37 H. J. Monkhorst and J. D. Pack, *Phys. Rev. B*, 1976, **13**, 5188–5192.

38 A. J. Ramirez-Cuesta, *Comput. Phys. Commun.*, 2004, **157**, 226–238.

39 M. D. Prasanna and T. N. G. Row, *J. Mol. Struct.*, 2001, **562**, 55–61.

40 D. E. Braun, *J. Pharm. Sci.*, 2013, **6**, 35–85.

41 N. A. Épshtein, *Pharm. Chem. J.*, 1995, **29**, 211–213.

42 G. J. Kearley, *Spectrochim. Acta Part A Mol. Spectrosc.*, 1992, **48**, 349–362.

43 H. N. Bordallo, B. A. Zakharov, E. V Boldyreva, M. R. Johnson, M. Marek Koza, T. Seydel and J. Fischer, *Mol. Pharm.*, 2012, **9**, 2434–2441.

44 M. Plazanet, A. Geis, M. R. Johnson and H. P. Trommsdorff, *J. Lumin.*, 2002, **98**, 197–205.

45 Jmol: an open-source Java viewer for chemical structures in 3D. http://www.jmol.org/.

46 J. R. Frisch, M.J., Trucks, G.W., Schlegel, H.B., Scuseria, G.E., Robb, M.A., Cheeseman, J. R., Gaussian 09, Revision B.01. (2010).

47 C. G. Don and S. Riniker, *J. Comput. Chem.*, 2014, **35**, 2279–2287.

48 F. Feixas, S. Lindert, W. Sinko and J. A. McCammon, *Biophys. Chem.*, 2014, **186**, 31–45.

49 J. Shonberg, R. C. Kling, P. Gmeiner and S. Löber, *Bioorg. Med. Chem.*, 2015, **23**, 3880–3906.

50 W. You, Y. M. Huang, S. Kizhake, A. Natarajan and C. A. Chang, *PLOS Comput. Biol.*, 2016, **12**, e1005057.

51 M. Salahinejad, T. C. Le and D. A. Winkler, *J. Chem. Inf. Model.*, 2013, **53**, 223–229.

52 NIST Chemistry WebBook, SRD 69, https://webbook.nist.gov/, (accessed 10 June 2019).

This journal is © The Royal Society of Chemistry 20xx

Please do not adjust margins

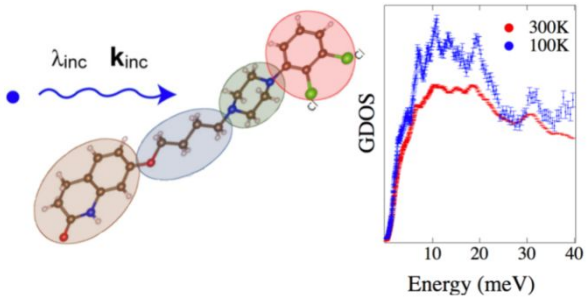

Deciphering the dynamics of the bioactive molecules using neutron spectroscopy to assist in the prediction of binding affinities.